Journal of Alloys and Compounds 508 (2010) 532–535

Contents lists available at ScienceDirect

Journal of Alloys and Compounds

journal homepage: www.elsevier.com/locate/jallcom

Nanocrystalline $SrHfO_3$ synthesized through a single step auto-igniting combustion technique and its characterization

J.K. Thomas[a,*], H. Padma Kumar[b], Sam Solomon[c], K.C. Mathai[a], J. Koshy[a]

[a] Electronic Materials Research Laboratory, Department of Physics, Mar Ivanios College, Thiruvananthapuram, Kerala 695 015, India
[b] Department of Physics, W.M.O Arts and Science College, Muttil, Wayanad, Kerala 673122, India
[c] Department of Physics, St. Johns College, Anchal, Kollam, Kerala 691306,India

ARTICLE INFO

Article history:
Received 8 May 2010
Received in revised form 11 August 2010
Accepted 26 August 2010
Available online 22 September 2010

Keywords:
Combustion synthesis
Ceramics
Nanoparticles
Materials processing

ABSTRACT

Nanocrystalline strontium hafnate ($SrHfO_3$) was synthesized through auto-ignited combustion technique. The X-ray diffraction studies of $SrHfO_3$ nanoparticles have shown that the as-prepared powder was single phase, crystalline, and has an orthorhombic (Pmna) perovskite structure (ABO_3). The phase purity of the powder was further examined using; thermo gravimetric analysis, differential thermal analysis, and Fourier transform infrared spectroscopy. The transmission electron microscopy study showed that the particle size of the as-prepared powder is in the range 20–60 nm with a mean size of 40 nm. The nanopowder could be sintered to 98% of the theoretical density at 1620 °C for 3 h. The microstructure of the sintered surface was examined using scanning electron microscopy. The dielectric constant (ε_r) of 25.13 and loss factor ($\tan\delta$) of 5.3×10^{-3} were obtained at 1 MHz.

1. Introduction

A wide range studies have been performed, predominantly during the past decade, on perovskite ceramics due to their excellent optical, electrical properties and intrinsic capability of hosting functional ions of various sizes [1,2]. Hafnium based perovskites ceramics have been of tremendous research interest in the recent past. The perovskite-type $BaHfO_3$, $SrHfO_3$, and other alkaline earth hafnates have been well known as high melting temperature materials [3,4]. Hafnium based perovskites doped with Yttrium has been reported as an interesting compound for their applications in fuel cells [5]. Perovskite structured hafnium compounds doped with various dopants were reported as good luminescent materials [6–8] and scintillating materials for their potential impact in high energy nuclear medical applications [9]. Recently $SrHfO_3$ was reported as a potential material for future CMOS technology [10]. Strontium based ABO_3 perovskites such as $SrZrO_3$ and $SrHfO_3$ adopts orthorhombic structures at room temperatures, undergoes a series of structural variation and becomes cubic at elevated temperatures [11]. Cuffini et al. [12] reported that $SrHfO_3$ is orthorhombic at room temperature, two phase transitions around 700 K (Pnma ↔ Imma) and around 1000 K (Imma ↔ Pm3m). Using powder neutron diffraction studies Kennedy et al. [13] reported that $SrHfO_3$ under goes three phase transitions. Accordingly $SrHfO_3$ is orthorhombic (Pmna) in the range 300–670 K, adopts a second orthorhombic phase transition (Cmcm) and tetragonal (14/mcm) in the region 1000–1353 K. At elevated temperatures (>1350 K) it becomes cubic ($Pm\bar{3}m$). Vali [14] have investigated the structural variations of seven phases for $SrHfO_3$ (Pnma, 14/mcm, Imma, Cmcm, P4/mbm, P4mm and $Pm\bar{3}m$) using density functional theory. The structural, mechanical and thermodynamic properties of seven phases of $SrHfO_3$ were studied by Liu et al. [15] using the plane wave ultrasoft pseudo-potential technique based on the first principles density functional theory. Thus a detailed study of the structural phase transition of $SrHfO_3$ is reported and in all the studies, $SrHfO_3$ possess an orthorhombic (Pnma) structure at room temperature. Generally conventional solid state ceramic route was used for the preparation of hafnia based compounds which requires prolonged calcination at about 1200 °C for several hours along with intermediate grinding in order to obtain reasonable phase purity. The coarse-grained powders synthesized using the conventional solid state route have the disadvantages of larger particle size, high temperature processing and lower phase purity [16,17]. A few reports are available on the preparation of $SrHfO_3$ such as laser heated pedestal growth [18], gel-combustion [19], anodic spark conversion [20] etc.

Synthesis of advanced ceramics and specialty materials as nanocrystals is one of the major challenges in the development of material processing technology. The advantages of nanocrystalline materials are superior phase homogeneity, sinterability and microstructure leading to unique mechanical, electrical, dielec-

* Corresponding author. Tel.: +91 471 2530887; fax: +91 471 2532445.
E-mail address: jkthomasemrl@yahoo.com (J.K. Thomas).

0925-8388/$ – see front matter © 2010 Elsevier B.V. All rights reserved.
doi:10.1016/j.jallcom.2010.08.112

tric, magnetic, optical and catalytic properties [21,22]. Recently a modified combustion synthesis technique was reported to be a better way in the preparation of advanced ceramics [23,24]. It was reported that by virtue of the different particle sizes and morphologies of the powders synthesized by the combustion technique [25], they show superior sintering behavior. In some ABO_3 perovskites based on zirconates, a reduction in sintering temperature of about 150 °C along with considerable reduction in sintering time was also observed [26–28]. The synthesis and characterization of double perovskites of some rare earth based barium hafnates are also reported for their superior sintering behavior [29–31]. In the present paper we are reporting the synthesis of $SrHfO_3$ as nanoparticles synthesized through a simple, economic auto-igniting single step combustion process and their subsequent characterization.

2. Experimental

In the present study a modified auto-igniting combustion technique [23,24] was used for the synthesis of nanoparticles of $SrHfO_3$. In a typical synthesis, aqueous solution containing ions of Sr and Hf were prepared by dissolving stoichiometric amount of high purity $Sr(NO_3)_2$ and $HfCl_4$ (99%) in double distilled water (200 ml) in a glass beaker. Citric acid (99%) was then added to the solution containing Sr and Hf ions. Amount of citric acid was calculated based on total valence of the oxidizing and the reducing agents for maximum release of energy during combustion [32]. Oxidant/fuel ratio of the system was adjusted by adding nitric acid and ammonium hydroxide and the ratio was kept at unity. The solution containing the precursor mixture at a pH of ~7.0 was heated using a hot plate at ~250 °C in a ventilated fume hood. The solution boils on heating and undergoes dehydration accompanied by foam. The foam then ignites by itself on persistent heating giving voluminous and fluffy product of combustion. The combustion product was subsequently characterized as single phase nanocrystals of $SrHfO_3$.

Structure of the as-prepared powder was examined by powder X-ray diffraction (XRD) technique using a X-ray diffractometer (Model Bruker D-8) with Nickel filtered CuK_α radiation. The differential thermal analysis (DTA) and thermo gravimetric Analyses (TGA) were carried out using Perkin-Elmer TG/DT thermal analyser in the range 30–1000 °C at a heating rate of 20 °C/min in nitrogen atmosphere. The infrared (IR) spectra of the samples were recorded in the range 400–4000 cm^{-1} on a Thermo-Nicolet Avatar 370 Fourier transform infrared (FT-IR) Spectrometer using KBr pellet method. Particulate properties of the combustion product were examined using transmission electron microscopy (Model: JEOL JEM 1011) at operating 200 kV. The samples for Transmission Electron Microscope (TEM) were prepared by ultrasonically dispersing the powder in methanol and allowing a drop of this to dry on a carbon-coated copper grid.

To study the sinterability of the nanoparticles obtained by the present combustion method, the as-prepared $SrHfO_3$ nanoparticles were mixed with 5% polyvinyl alcohol and pressed in the form of cylindrical pellet of 14 mm diameter and ~2 mm thickness at a pressure about 350 MPa using a hydraulic press. The pellet was then sintered at 1600 °C for 4 h. The theoretical density of the $SrHfO_3$ was calculated from the lattice constants and sintered density was calculated following Archimedes method.

The surface morphology of the sintered sample was examined using scanning electron microscopy (SEM, JEOL JSM 5610 LV).

3. Results and discussion

The XRD pattern taken at room temperature of the as-prepared powder obtained directly after combustion synthesis is shown in Fig. 1. All the peaks are indexed for orthorhombic perovskite (Pnma) structure and they agree very well with the reported XRD data for $SrHfO_3$ at room temperature (JCPDS 89-5606). The particle size calculated from full width half maximum (FWHM) using Scherrer formula for the major (1 2 1) reflection of Fig. 1 is found to be ~15 nm. No additional peaks correspond to any impurity phase was observed in the XRD pattern clearly show that the $SrHfO_3$ phase formation was complete during the combustion process itself without the need of further heating or calcination. It may be noted that a single phase materials can be obtained through solid state reaction route only after prolonged calcinations of the reaction mixture at 1200 °C with multiple intermediate grindings.

The thermal characterization of the as-prepared nanoparticles of $SrHfO_3$ synthesized through the combustion process was carried out using differential thermal analysis (DTA) and thermo gravimetric analysis (TGA) up to 1000 °C at heating rate of 10 °C/min. in nitrogen atmosphere. Fig. 2 shows the DTA and TGA curves of the as-prepared powders of $SrHfO_3$ obtained directly after combustion. The TGA curve shows a weight loss of 2% at about 100 °C, which can be due to the adsorbed moisture present in the sample. Thereafter there is a very small weight change of ~3% occurring in the sample at high temperatures up to 1000 °C, which implies that the combustion is complete and no considerable organic impurities are present in the sample. There is also no evidence of any considerable phase transition-taking place in the sample up to this temperature. Even though, $SrHfO_3$ undergoes phase variations from orthorhombic to cubic as discussed before, such transition are not so clear in a routine thermal analysis. Thus DTA and TGA analysis confirms the phase formation of $SrHfO_3$ in the combustion process itself.

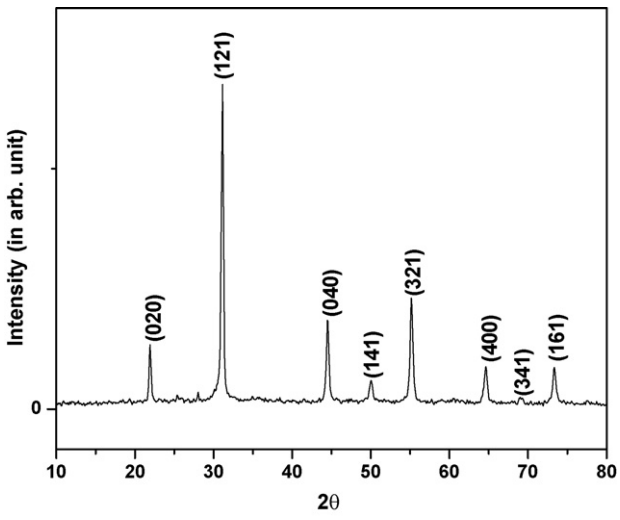

Fig. 1. XRD pattern of as-prepared $SrHfO_3$.

Fig. 3 shows the FT-IR spectrum of the typical as-prepared $SrHfO_3$ powder. The bands in FT-IR spectra are assigned mainly on the basis of vibrations of HfO_6 octahedra. The IR active $\gamma_3(F_{1u})$ asymmetric stretching mode of HfO_6 octahedra is observed as a strong absorption band at 565 cm^{-1}. The weak bands at 858 cm^{-1} is due to the Raman active symmetric stretching $\gamma_1(A_{1g})$ mode of HfO_6 octahedra [33,34]. The strong absorption band in the region 3000–3600 cm^{-1} is due to the symmetric stretching $\gamma_1(A_1)$ mode and asymmetric stretching $\gamma_3(F_2)$ mode of NH^{4+} ions in addition to the water adsorbed during pelletization. The bands at 1630 cm^{-1}

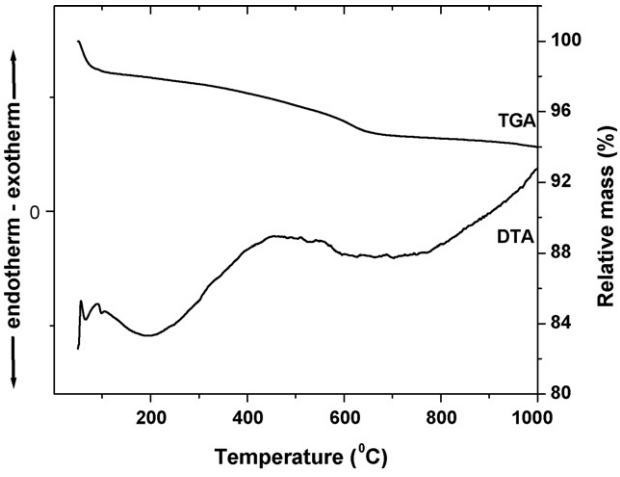

Fig. 2. DTA-TGA curves of as-prepared $SrHfO_3$.

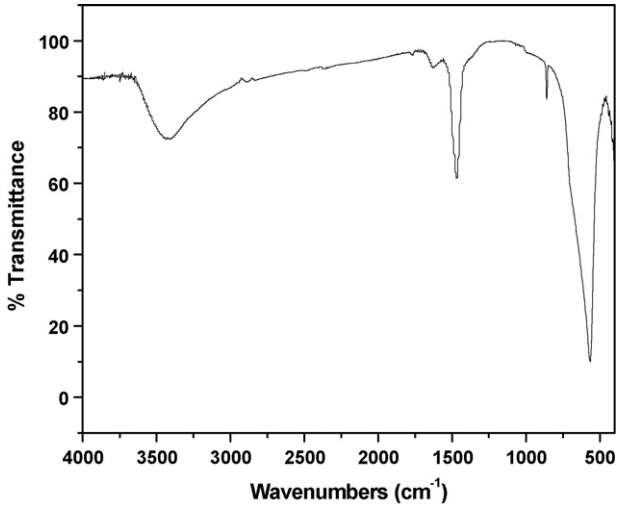

Fig. 3. FT-IR spectra of as-prepared $SrHfO_3$.

are due to the γ_2(E) bending modes of NH^{4+} ions. This corroborates the XRD and thermal analysis result that the combustion is complete and no considerable organic matter is present in the sample.

The transmission electron microscopy (TEM) studies on the powder morphology of the as-prepared $SrHfO_3$ nanopowder obtained by the combustion synthesis showed that the nanoparticles are of submicron size in the range 20–60 nm with a mean particle size of about 40 nm as shown in Fig. 4.It is by virtue that the combustion synthesis yield powders of varying particle size, due to the very short time duration of combustion and subsequent phase formation. The powder also shows ultra-fine nature attributed to the improved sinterability in comparison with their micro-structured coarse-grained counterparts. The corresponding selected area electron diffraction pattern is also shown in Fig. 4. The particles are of regular shape with sharp grain boundaries. Individual crystallites in the agglomerates appear well bonded with few voids in between. The ring nature of the Electron Diffraction Pattern is indicative of the poly crystalline nature of the crystallites, but the spotty nature of the SAD pattern in figure can be due to the fact that

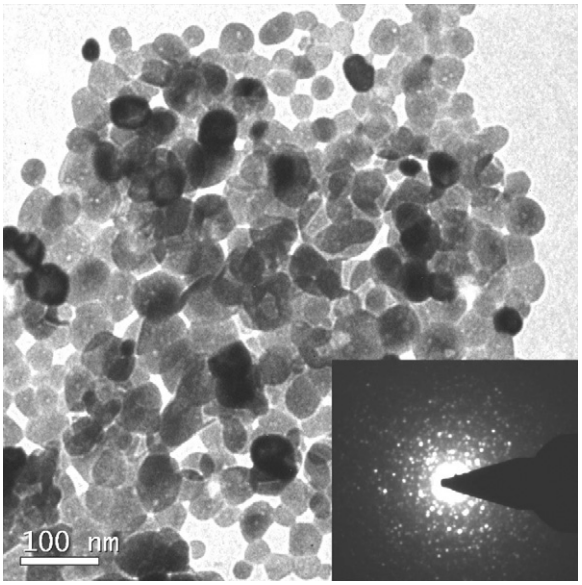

Fig. 4. TEM image of as-prepared $SrHfO_3$ (Inset-electron diffraction pattern).

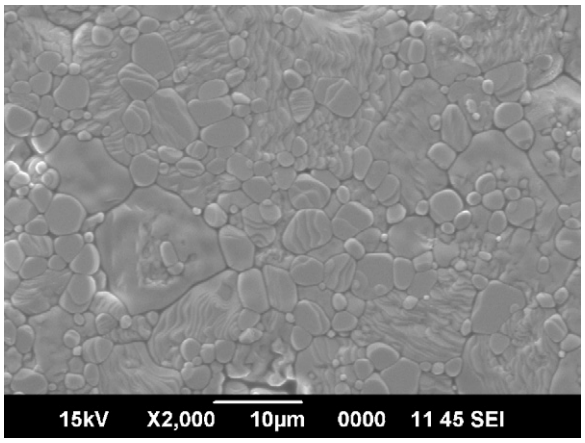

Fig. 5. SEM image of sintered $SrHfO_3$.

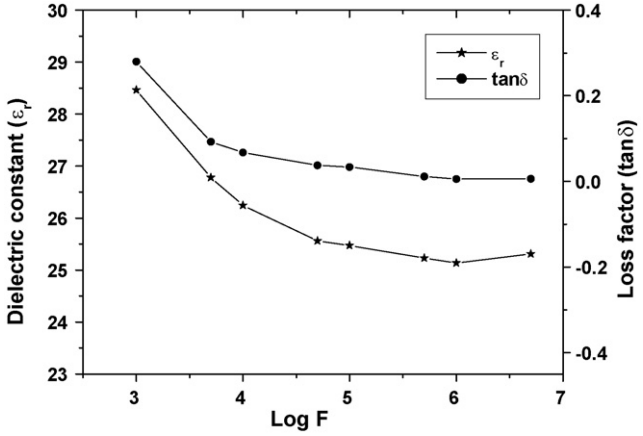

Fig. 6. Dielectric response of sintered $SrHfO_3$ pellet.

the finer crystallites having related orientations are agglomerated together resulting in a limited set of orientations.

The sintering behavior of the nanocrystals of $SrHfO_3$ powders synthesized through the present combustion route was studied. Fig. 5 shows the SEM image of sintered $SrHfO_3$. The relative green density of the specimen used for the sintering study was ~55%. A sintered density of about 98% of the theoretical density was obtained on sintering the compacted specimen at 1620 °C for 3 h. This high sintered density and the reduced temperature-time schedule is attributed to the enhanced kinetics due to the small degree of agglomeration and ultra-fine nature of $SrHfO_3$ prepared in the present study. No cracks or pores were observed on the surface. It is clear from the micrographs that densification was achieved without significant microstructural coarsening. Average grain size determined from the SEM micrographs is ~3 μm.

The variation of dielectric properties such as dielectric constant (ε_r) and loss factor ($\tan\delta$) with in the frequency range 1000 Hz to 5 MHz is shown in Fig. 6. The variation of dielectric constant with frequency is similar to that of the earlier reports of $SrHfO_3$ [35]. At about 1 MHz, a dielectric constant of 25.13 and loss factor of $\sim 5.3 \times 10^{-3}$ was obtained. The dielectric constant of sintered $SrHfO_3$ was found to be similar to that reported in the microwave region at about 9.3 GHz.

4. Conclusions

Synthesis, characterization, densification and dielectric properties of phase pure nanocrystalline $SrHfO_3$ (20–60 nm) powder

prepared by the modified combustion process are discussed. The X-ray diffraction studies of the nanoparticles of $SrHfO_3$ synthesized through the modified combustion route have shown that the as-prepared powder was single phase, crystalline and has an orthorhombic ABO_3 perovskite structure. The average particle size calculated from FWHM is ~15 nm. The phase purity of $SrHfO_3$ nanopowders has been confirmed using differential thermal analysis, thermo gravimetric analysis, and Fourier transform of infrared spectroscopy. The transmission electron microscopic investigation has shown that the particle size of the as-prepared powder was in the range 20–60 nm with a mean size of 40 nm. The thermal studies revealed that $SrHfO_3$ nanopowder was obtained in a single step process and no calcinations process was needed to obtain phase pure powder. The nanoparticles of $SrHfO_3$ obtained by the present combustion method were sintered to 98% of the theoretical density at a temperature of 1620 °C for 3 h. The dielectric constant (ε_r) of 25.13 and loss factor ($\tan\delta$) of 5.3×10^{-3} were obtained for the sintered $SrHfO_3$ pellets at 1 MHz measured at room temperature.

Acknowledgements

The authors acknowledge the financial support from, Kerala State Council for Science Technology& Environment, Government of Kerala, Trivandrum 695004 India.

References

[1] J.B. Goodenough, Rep. Prog. Phys. 67 (2004) 1915–1994.
[2] A.S. Bhalla, R. Guo, R. Roy, Mater. Res. Innovations 4 (2000) 3–26.
[3] P. Jorba, G. Tilloca, R. Collongues, Int. Symp. Magnetohydrodyn. Elec. Power Generation 3 (1964) 1185.
[4] N.D. Zhigadlo, P. Odier, J. Marty, ch. Bordet, P.A. Sulpice, Phys. C 387 (2003) 347–358.
[5] F.M.M. Snijkers, A. Buekenhoudt, J.J. Juyten, J. Cooymans, M. Mertens, Scripta Mater. 51 (2004) 1129–1134.
[6] H. Yamamoto, M. Mikami, Y. Shimomura, Y. Oguri, J. Lumin. 87–89 (2000) 1079–1082.
[7] N. Arai, T.W. Kim, H. Kubota, Y. Matsumoto, H. Koinuma, Appl. Surf. Sci. 197–198 (2002) 402–405.
[8] W.J. Schipper, J.J. Piet, H.J. De Jager, G. Blasse, Mater. Res. Bull. 29 (1) (1994) 23–30.
[9] S.L. Dole, S. Venkataramani, U.S. Patent #5124072.
[10] C. Rossel, M. Sousa, C. Marchiori, J. Fompeyrine, D. Webb, D. Caimi, B. Mereu, A. Ispas, J.P. Locquet, H. Siegwart, R. Germann, A. Tapponnier, K. Babich, Microelectron. Eng. 84 (2007) 1869–1873.
[11] S. Hasegawa, T. Sugimoto, T. Hashimoto, Solid State Ionics 181 (2010) 1091–1097.
[12] S. Cuffini, J.A. Guevara, Y.P. Mascarenhas, P. De La Presa, A. Ayala, A. Lopez Garcia, Ceramica 43 (1997) 91–94.
[13] B.J. Kennedy, C.J. Howard, B.C. Chakoumakos, Phys. Rev. B 60 (1999) 2972–2975.
[14] R. Vali, Solid State Commun. 148 (2008) 29–31.
[15] Q.J. Liu, Z.T. Liu, L.P. Feng, H. Tian, L. Liu, W.T. Liu, Comput. Mater. Sci. 48 (2010) 677–679.
[16] J.K. Thomas, J. Koshy, Int. J. Inorg. Mater. 3 (2001) 737–741.
[17] J. Koshy, J.K. Thomas, J. Kurian, Y.P. Yadava, A.D. Damodaran, Mater. Lett. 15 (1992) 298–301.
[18] M.R.B. Andreeta, A.C. Hernandes, S.L. Cuffini, J.A. Guevara, Y.P. Mascarenhas, J. Cryst. Growth (1999) 621–624.
[19] Y.M. Ji, D.Y. Jiang, Z.H. Wu, T. Feng, J.L. Shi, Mater. Res. Bull. 40 (2005) 1521–1526.
[20] J.P. Schreckenbach, N. Meyer, G. Marx, B.T. Lee, W.M. Kriven, Appl. Surf. Sci. 205 (2003) 97–101.
[21] H. Gleiter, Acta Mater. 48 (2000) 1–29.
[22] C. Suryanarayana, Bull. Mater. Sci. 17 (4) (1994) 307–346.
[23] J. James, R. Jose, A.M. John, J. Koshy, US Patent No. 6,761,866 July 13 (2004).
[24] J. James, R. Jose, A.M. John, J. Koshy, US Patent No.6,835,367 December 28 (2004).
[25] I. Robert, L. Radu, Mater. Chem. Phys. 115 (2009) 645–648.
[26] H. Padma Kumar, C. Vijayakumar, C.N. George, S. Solomon, R. Jose, J.K. Thomas, J. Koshy, J. Alloys Compd. 458 (2008) 528–531.
[27] J.K. Thomas, H. Padma Kumar, R. Pazhani, S. Solomon, R. Jose, J. Koshy, Mater. Lett. 61 (2006) 1592–1595.
[28] C.S. Prasanth, H. Padma Kumar, R. Pazhani, S. Solomon, J.K. Thomas, J. Alloys Compd. 464 (2008) 306–309.
[29] J.K. Thomas, H. Padma Kumar, S. Solomon, C.N. George, K. Joy, J. Koshy, Physica Status Solidi (a) 204 (9) (2007) 3102–3107.
[30] J.K. Thomas, H. Padma Kumar, A. John, V. Suni, K. Joy, S. Solomon, J. Koshy, J. Phys. Chem. Solids 70 (2009) 703–706.
[31] A.M. John, R. Jose, J. Koshy, J. Nanopart. Res. 3 (2001) 411–415.
[32] R.C. Patil, S. Radhakrishnan, S. Pethkar, K. Vijaymohan, J. Mater. Res. 16 (2001) 1982–1988.
[33] A.E. Lavat, E.J. Baran, Vib. Spectrosc. 32 (2003) 167–174.
[34] W. Zheng, W. Pang, G. Meng, Mater. Lett. 37 (1998) 276–280.
[35] A. Feteira, D.S. Sinclair, R.Z. Khalid, M.T. Lanagan, J. Am. Ceram. Soc. 91 (2008) 893–901.